

Thermal Transport and Phonon Hydrodynamics in Strontium Titanate

Valentina Martelli,¹ Julio Larrea Jiménez,² Mucio Continentino,¹ Elisa Baggio-Saitovitch,¹ and Kamran Behnia^{3,4}

¹*Centro Brasileiro de Pesquisas Físicas, 22290-180 Rio de Janeiro, Rio de Janeiro, Brazil*

²*Institute of Physics, University of São Paulo, CEP 05508-090 São Paulo, São Paulo, Brazil*

³*Laboratoire Physique et Etude de Matériaux (CNRS-UPMC), ESPCI Paris, PSL Research University, 75005 Paris, France*

⁴*II. Physikalisches Institut, Universität zu Köln, 50937 Köln, Germany*



(Received 7 December 2017; published 22 March 2018)

We present a study of thermal conductivity, κ , in undoped and doped strontium titanate in a wide temperature range (2–400 K) and detecting different regimes of heat flow. In undoped SrTiO₃, κ evolves faster than cubic with temperature below its peak and in a narrow temperature window. Such behavior, previously observed in a handful of solids, has been attributed to a Poiseuille flow of phonons, expected to arise when momentum-conserving scattering events outweigh momentum-degrading ones. The effect disappears in the presence of dopants. In SrTi_{1-x}Nb_xO₃, a significant reduction in lattice thermal conductivity starts below the temperature at which the average inter-dopant distance and the thermal wavelength of acoustic phonons become comparable. In the high-temperature regime, thermal diffusivity becomes proportional to the inverse of temperature, with a prefactor set by sound velocity and Planckian time ($\tau_p = (\hbar/k_B T)$).

DOI: [10.1103/PhysRevLett.120.125901](https://doi.org/10.1103/PhysRevLett.120.125901)

Heat travels in insulators thanks to phonons. This has been described by the Peierls-Boltzmann equation, which quantifies the spatial variation in phonon population caused by the temperature gradient. In recent years, thanks to improved computing performance and new theoretical techniques, a quantitative account of the intrinsic thermal conductivity of semiconductors is accessible to first-principles theory [1]. When most scattering events conserve momentum and do not decay heat flux, collective phonon excitations, dubbed relaxons, become fundamental heat carriers [2]. This hydrodynamic regime of phonon flow, identified decades ago [3–6], is gaining renewed attention in the context of graphene-like two-dimensional systems [7,8].

The perovskite SrTiO₃ is a quantum paraelectric [9], which owes its very existence to zero-point quantum fluctuations. First-principles calculations find imaginary phonon modes [10], which hinder a quantitative understanding of the lattice thermal transport [11]. This insulator turns to a metal upon the introduction of a tiny concentration of dopants. The metal has a dilute superconducting ground state [12] and an intriguing room-temperature charge transport [13]. Its thermal conductivity has remained largely unexplored, in contrast to electric [14] and thermoelectric [15] transport.

In this Letter, we present an extensive study of the thermal conductivity, κ , of undoped and doped SrTiO₃ crystals and report on three new findings. First of all, in a narrow temperature range, thermal conductivity evolves faster than cubic. This behavior had only been reported in a handful of solids [6] and attributed to a Poiseuille flow of phonons. We argue that the emergence of phonon

hydrodynamics results from the multiplication of momentum-conserving scattering events due to the presence of a ferroelectric soft mode, as suggested decades ago [16]. This interpretation lends support to previous reports on the observation of the second sound in this system [17,18], which has been controversial [19]. Second, our study finds that a random distribution of dopants drastically reduces thermal conductivity below a temperature which tunes the heat-carrying phonon wavelength to the average inter-dopant distance. Finally, we put under scrutiny the thermal diffusivity of the system near room temperature and link its magnitude and temperature dependence to the so-called Planckian scattering time [20], in the context of the ongoing debate on a possible boundary to diffusivity [21,22].

The cubic elementary cell of strontium titanate encloses a TiO₆ octahedra and has strontium atoms at its vertices [Fig. 1(a)]. Neutron and Raman scattering studies have identified two distinct soft modes. The first is associated with the antiferrodistortive (AFD) transition, which leads to the loss of cubic symmetry at 105 K [23] by tilting two adjacent TiO₆ octahedra in opposite orientations. It is centered at the *R* point of the Brillouin zone [Fig. 1(b)]. The second soft mode [24], located at the zone center, is associated with the aborted ferroelectricity. Figure 1(c) presents the temperature dependence of the two modes established by converging spectroscopic tools [23,25,26]. In common solids, only acoustic branches can host thermally excited phonons at low temperatures. Here, phonons associated with these soft modes remain relevant down to fairly low temperatures.

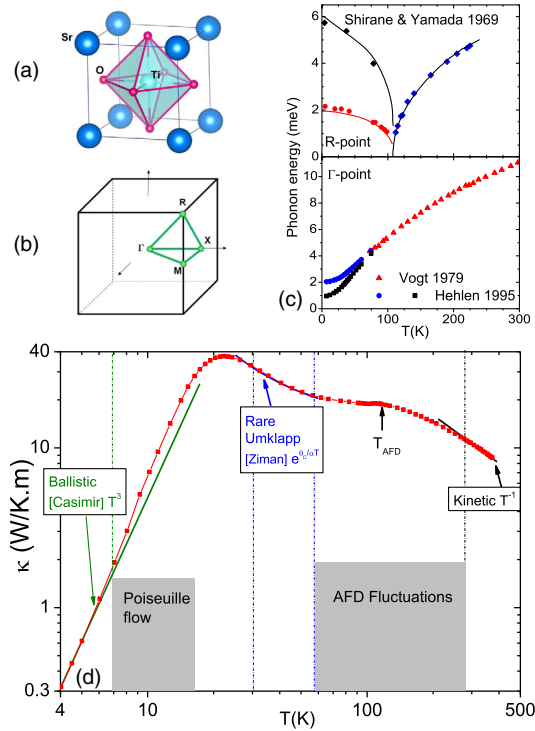


FIG. 1. (a) Crystal structure of strontium titanate. (b) The cubic Brillouin zone and its high-symmetry points. (c) The temperature dependence of the two soft modes according to neutron scattering studies [23] and hyper-Raman [25] and Brillouin scattering spectroscopy [26]. (d) Thermal conductivity of a SrTiO₃ crystal (closed red squares) in a log-log plot [for a linear plot, see Fig. 3(a)]. Different regimes of thermal transport are identified. Solid lines represent the expected behaviors in these regimes. An additional window due to enhanced umklapp scattering opens up in the vicinity of the antiferrodistortive (AFD) transition.

We used a standard one-heater, two-thermometers technique to measure the thermal conductivity of commercial single crystal of Sr_{1-x}Nb_xTiO₃ (see the Supplemental Material [27]). The results, presented in Fig. 1(d), reveal different regimes of heat transport classified by previous authors [4,6,8]. Simply put, thermal conductivity is the product of specific heat, mean free path, and velocity [33]. At one extreme, i.e., at low temperature, the phonon mean free path saturates, the system enters the ballistic regime, and κ becomes cubic in temperature. In the other extreme, at high temperature, the specific heat saturates and thermal conductivity, reflecting the temperature dependence of the mean free path, follows T^{-1} . In this kinetic regime, the wave vector of thermally excited phonons is large enough to allow umklapp scattering events. Well below the Debye temperature, such events become rare and κ increases exponentially. This is the Ziman regime.

The AFD transition has visible consequences for heat transport. First of all, it attenuates κ near T_{AFD} , impeding a smooth evolution between T^{-1} and exponential regimes. The R-point soft mode associated with the AFD transition

provides additional umklapp scattering at low energy cost. Interestingly, fitting $\kappa \propto \exp[(E_D/T)]$ in the Ziman regime, one finds $E_D \simeq 20$ K, an energy scale comparable to the AFD soft mode. The second consequence of the AFD transition is to generate multiple tetragonal domains in an unstrained crystal [34]. Given that the typical size of tetragonal domains is a few microns [35], the upper boundary to the ballistic mean free path of phonons can be much lower than it is in the sample dimensions.

We found a κ varying faster than T^3 in a narrow (6 K < T < 13 K) temperature window just below the peak. Usually, the ballistic regime ends with a downward deviation of κ from its cubic temperature dependence. This happens in silicon [36] [Fig. 2(a)] or in KTaO₃ [Fig. 2(b)]. This is not the case in bismuth, where it shows an upward deviation between the ballistic regime and the peak [Fig. 2(c)]. This has been identified as a signature of a Poiseuille flow of phonons [37].

The Poiseuille regime emerges when energy exchange between phonons is frequent enough to keep the local temperature well defined, and umklapp collisions are so rare that the flow is mainly impeded by boundary

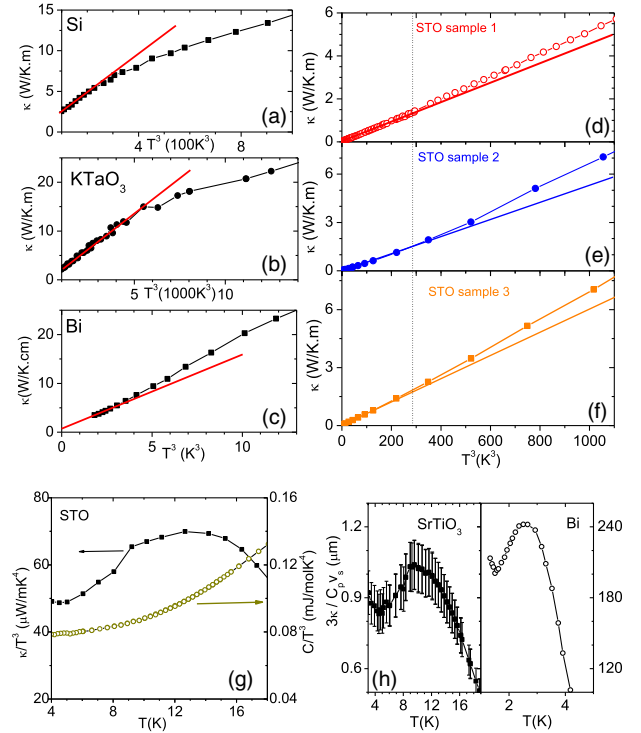


FIG. 2. Thermal conductivity, κ , as a function of T^3 , (a) in silicon (after Ref. [36]) and (b) in KTaO₃. In both, κ deviates downward from the T^3 line. (c) In bismuth (after Ref. [37]), it deviates upward. (d–f) In three different crystals of SrTiO₃, the deviation is upward. (g) The thermal conductivity and specific heat of SrTiO₃ evolve faster than cubic in this temperature range. But in a narrow window, thermal conductivity increases more rapidly. (h) The apparent mean free path in both Bi and SrTiO₃ present a local peak, the hallmark of Poiseuille flow.

scattering. Without viscosity, no external temperature gradient would be then required to sustain the phonon drift [5]. This picture, developed decades ago [3–5], requires a hierarchy of time scales. The time separating two normal scattering events, τ_N , should become much shorter than the time between boundary scattering events, τ_B , and the latter much shorter than the time between resistive scattering events, τ_R , which are due to either umklapp or impurity scattering. The same hierarchy ($\tau_N \ll \tau_B \ll \tau_R$) is required for second sound, a wavelike propagation of temperature and entropy, which has been observed in bismuth as well as in other solids displaying Poiseuille flow [6].

We confirmed a faster-than-cubic κ in three different SrTiO₃ crystals [Figs. 2(d)–2(f)]. Here, the identification of this behavior with Poiseuille flow is less straightforward, since the specific heat of SrTiO₃ also evolves faster than cubic between 4 K and 20 K [38]. This is because the Debye approximation is inadequate in the presence of soft modes, and one needs to consider Einstein terms of the soft optical modes. In order to address this concern, we measured the specific heat of our cleanest crystal and found that the thermal conductivity increases faster than the specific heat [Fig. 2(g)]. The effective phonon mean free path, $\ell_{ph} = (3\kappa C_p/v_s)$, extracted from the specific heat, C_p , and the sound velocity, v_s , was found to show a peak comparable to what was found in bismuth [37] [Fig. 2(h)]. In both cases, ℓ_{ph} presents a local maximum 1.3 times the Knudsen minimum. The magnitude of the latter is slightly smaller than the crystal dimensions in bismuth, and similar to the typical size of tetragonal domains in strontium titanate, which have been found to be of the order of a micrometer [35]. As far as we know, the only available explanation for a local peak in ℓ_{ph} is Poiseuille flow.

Neither in bismuth nor in strontium titanate is the chemical purity exceptionally high. The same is true of black phosphorus, where a faster-than-cubic κ was recently observed [39]. Therefore, in these cases, in contrast to He crystals, the Poiseuille flow is presumably caused by a large three-phonon phase space [40] for momentum-conserving (compared to momentum-degrading) scattering events. We note that the low-temperature validity of the $\tau_N \ll \tau_R$ inequality in strontium titanate was previously confirmed by low-frequency light scattering experiments [18]. Anomalies detected by Brillouin scattering experiments [26] are believed to be caused by strong anharmonic coupling between acoustic and optical modes at low temperatures. A strong hybridization between acoustic and transverse optical phonons was theoretically confirmed [41] and is expected to flatten the phonon dispersion. This would pave the way for frequent normal momentum exchange. It would also pull down the phonon velocity, providing an alternative explanation for an unusually short apparent mean free path.

Let us turn our attention to the effect of atomic substitution. Figure 3(a) shows the thermal conductivity

of SrTi_{1-x}Nb_xO₃. The magnitude of κ smoothly decreases with increasing dopant concentration. Only at lower temperatures, additional contribution by electrons outweighs the reduction in lattice thermal conductivity. In this range, we resolve a finite- T linear component in thermal conductivity of metallic samples due to the electronic component of thermal conductivity, κ_e . This is in agreement with a previous study focused on temperatures below 0.5 K [42], which verified the validity of the Wiedemann-Franz (WF) law in the zero-temperature limit, namely $\kappa_e \rho/T = L_0$, where ρ is the electric resistivity and $L_0 = 2.45 \times 10^{-8} \text{ V}^2/\text{K}^2$ is the Lorenz number. Assuming the validity of the WF law at finite temperatures, one can separate the electronic, κ_e , and the phononic, κ_{ph} , components of the total thermal conductivity. At finite temperature, because of inelastic scattering, one expects $\kappa_e \rho/T L_0 \leq 1$ and electric resistivity provides only a rough measure of κ_e , which, as seen in Fig. 3(b), becomes rapidly much smaller than κ_{ph} with rising temperature.

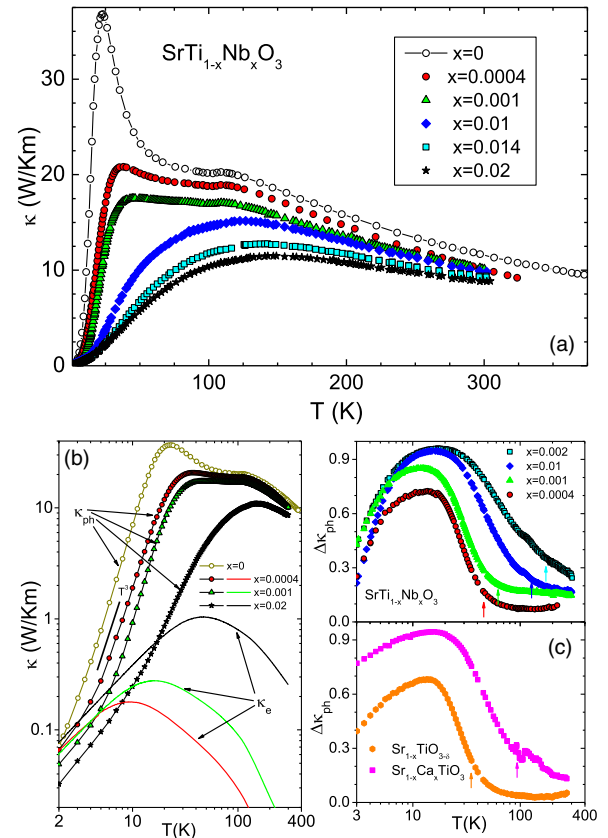


FIG. 3. (a) κ as a function of temperature in SrTi_{1-x}Nb_xO₃. (b) Electronic, κ_e and phononic, κ_{ph} , components of the thermal conductivity in three doped samples compared to undoped strontium titanate. Note the persistence of a T^3 behavior over a wide temperature window with a drastically reduced magnitude. (c) Relative attenuation in phonon thermal conductivity, $\Delta\kappa_{ph} = 1 - (\kappa_{ph}(x \neq 0)/\kappa_{ph}(x=0))$ in SrTi_{1-x}Nb_xO₃ (top) and in Sr_{1-x}Ca_xTiO₃ ($x = 0.0045$) and in SrTiO_{3- δ} ($n = 7 \times 10^{17} \text{ cm}^{-3}$). Small arrows represent T_{qn} (See text).

The first consequence of the disorder, introduced by this tiny substitution for κ_{ph} , is the loss of the faster-than-cubic regime associated with Poiseuille flow. As seen in Fig. 3(b), reminiscent of what was observed in doped silicon and germanium [43], doping drastically damps κ_{ph} at low temperatures. The temperature dependence of the attenuation of phonon thermal conductivity caused by substitution, $\Delta\kappa_{\text{ph}} = 1 - \kappa_{\text{ph}}(x \neq 0)/\kappa_{\text{ph}}(x = 0)$, presented in Fig. 3(c), displays a regular pattern. For a small substitution ($x = 0.0004$), the lattice thermal conductivity is reduced by 8% at room temperature, by as much as 70% at 20 K, and by 20% at 3 K. In other words, the maximum attenuation occurs in an intermediate temperature window. With increasing Nb concentration, the pattern is similar, but it shifts to higher temperatures. As seen in the lower panel of Fig. 3(c), our measurements on an oxygen-reduced and a calcium-substituted sample produce similar patterns. Since Ca substitution [44] keeps the system an insulator, one can conclude that the drastic reduction in lattice conductivity is mainly due to the random distribution of substituting atoms and *not* to the scattering by mobile electrons.

A rigorous account of the temperature dependence of $\Delta\kappa_{\text{ph}}$ is missing. We note, however, that $\Delta\kappa_{\text{ph}}$ drastically enhances at a temperature which shifts upward as the concentration increases [see upward arrows in Fig. 3(c)]. Consider that with decreasing temperature, the typical wave vector of thermally excited phonons shrinks, following $q_{\text{ph}} = (k_B T / \hbar v_s)$. Therefore, at high temperature, the phonon wavelength is shorter than the average distance between dopants, and the effect of disorder is limited. The random distribution of dopants begins to matter when the phonon wavelength becomes comparable to the average interdopant distance. In contrast to electrons, Anderson localization of phonons [45] is not expected to impede diffusive transport [46]. Theoretically, a tiny level of disorder is sufficient to transform some phonon modes from propagating waves (propagons) to diffusons, which travel diffusively, or to fully localized locons [47]. One expects phonons with a wavelength much shorter or much longer than the randomness length to be less affected. As a consequence, attenuation is to be more pronounced in the temperature window where the most concerned phonons happen to be dominant thermally excited carriers of heat. For each concentration, n , a temperature, $T_{qn} = \hbar v_s / \ell_{dd} k_B$, can be defined, which corresponds to equality between the typical acoustic phonon wavelength, $\lambda_{\text{ph}} = 2\pi/q_{\text{ph}}$, and interdopant distance, $\ell_{dd} = n^{-1/3}$. As one can see in Fig. 3(c), T_{qn} is close to where $\Delta\kappa_{\text{ph}}$ becomes large. Such a crude picture based on the Debye approximation should not be taken too literally in the presence of soft modes.

In principle, *ab initio* calculations [1] can give an account of heat transport near room temperature. Recently, two groups [48,49] succeeded in determining

the phonon spectrum of strontium titanate free of the commonly found imaginary frequencies [10] and in computing the intrinsic lattice conductivity of the cubic phase. Figure 4(a) compares our high-temperature data with these calculations [48,49] as well as previous experimental reports [11,50,51]. As one can see in the figure, there is broad agreement between experimental results. Theoretical calculations using the generalized gradient approximation (GGA) [48] are very close to the experimental data above 250 K. On the other hand, the experimental slope matches more the theory based on microscopic anharmonic force constants [49].

Let us conclude with a short discussion of thermal diffusivity, $D = (\kappa/C_p)$ in this regime. We can extract D by combining our thermal conductivity data and the specific heat. Figure 4(b) presents the temperature dependence of thermal diffusivity. One can see that, at room temperature and above, thermal diffusivity tends to be proportional to T^{-1} . Our data are in good agreement with reported values of thermal diffusivity at high temperatures [52]. In the vicinity of room temperature and above, thermal diffusivity becomes proportional to the inverse of temperature. The thermal diffusivity of a good conductor of heat, silicon, and a very bad one, PbTe, are also shown.

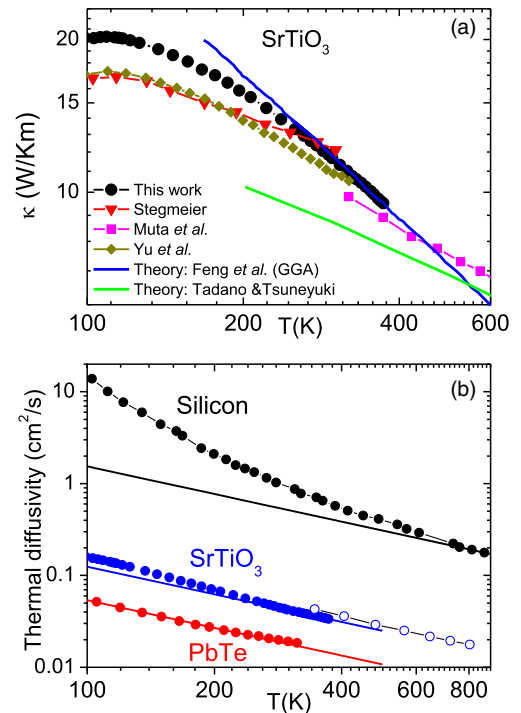


FIG. 4. (a) Thermal conductivity at high temperatures compared to previous experimental reports [11,50,51] and theoretical calculations [48,49]. (b) Thermal diffusivity, D , extracted from thermal conductivity and specific heat data as a function of temperature in SrTiO_3 (solid blue circles) together with data from Ref. [52] (open circles), compared to silicon and PbTe. Solid lines represent $D = sv_s^2\tau_p$ (see text).

TABLE I. Room-temperature thermal diffusivity ($D_{300\text{ K}}$), longitudinal sound velocity (v_{sl}), and the parameter s quantifying the slope of high-temperature thermal diffusivity, in three cubic solids.

System	$D_{300\text{ K}}$ (mm ² /s)	v_{sl} (100)(km/s)	s
SrTiO ₃	4.0	7.87	2.6
PbTe	1.9	3.59	5.9
Si	91	8.43	51

Remarkably, in the two bad conductors, the magnitude and the temperature dependence of D in the high-temperature regime can be expressed in a very simple way:

$$D = sv_s^2\tau_p. \quad (1)$$

Here, $\tau_p = (\hbar/k_B T)$ is the Planckian scattering time [20], and s is a dimensionless parameter (see Table I). In PbTe and SrTiO₃, s is close to unity, and the temperature dependence is set by τ_p . It emerges as a useful parameter for comparing the thermal conductivity of different cubic insulators. In many perovskites, recently studied by Hofmeister [52], D has a comparable magnitude and temperature dependence. On the other hand, in a highly conducting cubic insulator such as silicon, D is much larger and drops faster, presumably because the phase space for three-phonon scattering umklapp events [40] is smaller.

Equation (1) is strikingly similar to the universal boundary on diffusivity suggested by Hartnoll [21], with sound velocity replacing the Fermi velocity. The experimental motivation for Hartnoll's proposal [21] was the fact that τ_p is the average scattering rate of electrons in numerous metals with linear resistivity [20]. Is there a boundary to thermal transport by phonons in insulators? In other words, is there a fundamental reason for s to remain larger than unity? These are the questions raised by our observation.

J. L. J. acknowledges the Science Without Borders program of CNPq/MCTI-Brazil, and V. M. and K. B. acknowledge FAPERJ fellowships (Nota 10 and Visitante). K. B. is also supported by Fonds ESPCI and by a QuantEmX Grant (No. GBMF5305) from ICAM and the Gordon and Betty Moore Foundation. We thank B. Fauqué, Y. Fuseya, S. A. Hartnoll, and A. Kapitulnik for stimulating discussions.

- [1] L. Lindsay, D. A. Broido, and T. L. Reinecke, *Phys. Rev. B* **87**, 165201 (2013).
 [2] A. Cepellotti and N. Marzari, *Phys. Rev. X* **6**, 041013 (2016).
 [3] J. A. Sussmann and A. Thellung, *Proc. Phys. Soc.* **81**, 1122 (1963).
 [4] R. A. Guyer and J. A. Krumhansl, *Phys. Rev.* **148**, 778 (1966).

- [5] R. N. Gurzhi, *Sov. Phys. Usp.* **11**, 255 (1968).
 [6] H. Beck, P. F. Meier, and A. Thellung, *Phys. Status Solidi (a)* **24**, 11 (1974).
 [7] A. Cepellotti, G. Fugallo, L. Paulatto, M. Lazzeri, F. Mauri, and N. Marzari, *Nat. Commun.* **6**, 6400 (2015).
 [8] S. Lee, D. Broido, K. Esfarjani, and G. Chen, *Nat. Commun.* **6**, 6290 (2015).
 [9] K. A. Müller and H. Burkard, *Phys. Rev. B* **19**, 3593 (1979).
 [10] U. Aschauer and N. A. Spaldin, *J. Phys. Condens. Matter* **26**, 122203 (2014).
 [11] E. F. Steigmeier, *Phys. Rev.* **168**, 523 (1968).
 [12] X. Lin, Z. Zhu, B. Fauqué, and K. Behnia, *Phys. Rev. X* **3**, 021002 (2013).
 [13] X. Lin, C. W. Rischau, L. Buchauer, A. Jaoui, B. Fauqué, and K. Behnia, *npj Quantum Mater.* **2**, 41 (2017).
 [14] X. Lin, B. Fauqué, and K. Behnia, *Science* **349**, 945 (2015).
 [15] T. A. Cain, A. P. Kajdos, and S. Stemmer, *Appl. Phys. Lett.* **102**, 182101 (2013).
 [16] V. L. Gurevich and A. K. Tagantsev, *J. Exp. Theor. Phys.* **67**, 206 (1988).
 [17] B. Hehlen, A. L. Pérou, E. Courtens, and R. Vacher, *Phys. Rev. Lett.* **75**, 2416 (1995).
 [18] A. Koreeda, R. Takanao, and S. Saikan, *Phys. Rev. Lett.* **99**, 265502 (2007).
 [19] J. F. Scott, A. Chen, and H. Ledbetter, *J. Phys. Chem. Solids* **61**, 185 (2000).
 [20] J. A. N. Bruin, H. Sakai, R. S. Perry, and A. P. Mackenzie, *Science* **339**, 804 (2013).
 [21] S. A. Hartnoll, *Nat. Phys.* **11**, 54 (2015).
 [22] J. Zhang, E. M. Levenson-Falk, B. J. Ramshaw, D. A. Bonn, R. Liang, W. N. Hardy, S. A. Hartnoll, and A. Kapitulnik, *Proc. Natl. Acad. Sci. U.S.A.* **114**, 5378 (2017).
 [23] G. Shirane and Y. Yamada, *Phys. Rev.* **177**, 858 (1969).
 [24] Y. Yamada and G. Shirane, *J. Phys. Soc. Jpn.* **26**, 396 (1969).
 [25] H. Vogt, *Phys. Rev. B* **51**, 8046 (1995).
 [26] B. Hehlen, L. Arzel, A. K. Tagantsev, E. Courtens, Y. Inaba, A. Yamanaka, and K. Inoue, *Physica (Amsterdam)* **263B–264B**, 627 (1999).
 [27] See Supplemental Material at <http://link.aps.org/supplemental/10.1103/PhysRevLett.120.125901> for methods and details, which includes Refs. [28–32].
 [28] A. Spinelli, M. A. Torija, C. Liu, C. Jan, and C. Leighton, *Phys. Rev. B* **81**, 155110 (2010).
 [29] P. D. Desai, *J. Phys. Chem Ref. Data* **15**, 967 (1985).
 [30] D. H. Parkinson and J. E. Quarrington, *Proc. Phys. Soc.* **67**, 569 (1954).
 [31] A. S. Pashinkin *et al.*, *Inorg. Mater.* **45**, 1226 (2009).
 [32] D. T. Morelli, V. Jovicic, and J. P. Heremans, *Phys. Rev. Lett.* **101**, 035901 (2008).
 [33] R. Berman, *Thermal Conduction in Solids*, (Oxford University, New York, 1976).
 [34] Q. Tao, B. Loret, B. Xu, X. Yang, C. W. Rischau, X. Lin, B. Fauqué, M. J. Verstraete, and K. Behnia, *Phys. Rev. B* **94**, 035111 (2016).
 [35] A. Buckley, J. P. Rivera, and E. K. H. Salje, *J. Appl. Phys.* **86**, 1653 (1999).
 [36] C. J. Glassbrenner and G. A. Slack, *Phys. Rev.* **134**, A1058 (1964).

- [37] V.N. Kopylov and L.P. Mezhov-Deglin, *J. Exp. Theor. Phys.* **38**, 357 (1974).
- [38] M. Ahrens, R. Merkle, B. Rahmati, and J. Maier, *Physica (Amsterdam)* **393B**, 239 (2007).
- [39] Y. Machida *et al.*, [arXiv:1802.05867](https://arxiv.org/abs/1802.05867).
- [40] L. Lindsay and D. A. Broido, *J. Phys. Condens. Matter* **20**, 165209 (2008).
- [41] A. Bussmann-Holder, *Phys. Rev. B* **56**, 10762 (1997).
- [42] X. Lin, A. Gourgout, G. Bridoux, F. Jomard, A. Pourret, B. Fauqué, D. Aoki, and K. Behnia, *Phys. Rev. B* **90**, 140508 (R) (2014).
- [43] J. A. Carruthers, T. H. Geballe, H. M. Rosenberg, and J. M. Ziman, *Proc. R. Soc. A* **238**, 502 (1957).
- [44] C. W. Rischau *et al.*, *Nat. Phys.* **13**, 643 (2017).
- [45] M. N. Luckyanova *et al.*, [arXiv:1602.05057](https://arxiv.org/abs/1602.05057).
- [46] P. Sheng, M. Zhou, and Z.-Q. Zhang, *Phys. Rev. Lett.* **72**, 234 (1994).
- [47] H. R. Seyf and A. Henry, *J. Appl. Phys.* **120**, 025101 (2016).
- [48] L. Feng, T. Shiga, and J. Shiomi, *Appl. Phys. Express* **8**, 071501 (2015).
- [49] T. Tadano and S. Tsuneyuki, *Phys. Rev. B* **92**, 054301 (2015).
- [50] H. Muta, K. Kurosaki, and S. Yamanaka, *J. Alloys Compd.* **392**, 306 (2005).
- [51] C. Yu, M. L. Scullin, M. Huijben, R. Ramesh, and A. Majumdar, *Appl. Phys. Lett.* **92**, 191911 (2008).
- [52] A. M. Hofmeister, *J. Appl. Phys.* **107**, 103532 (2010).